

NASA/TM—2005–213609



# **Safe Affordable Fission Engine- (SAFE-) 100a Heat Exchanger Thermal and Structural Analysis**

*B.E. Steeve*

*Marshall Space Flight Center, Marshall Space Flight Center, Alabama*

---

**March 2005**

## The NASA STI Program Office...in Profile

Since its founding, NASA has been dedicated to the advancement of aeronautics and space science. The NASA Scientific and Technical Information (STI) Program Office plays a key part in helping NASA maintain this important role.

The NASA STI Program Office is operated by Langley Research Center, the lead center for NASA's scientific and technical information. The NASA STI Program Office provides access to the NASA STI Database, the largest collection of aeronautical and space science STI in the world. The Program Office is also NASA's institutional mechanism for disseminating the results of its research and development activities. These results are published by NASA in the NASA STI Report Series, which includes the following report types:

- **TECHNICAL PUBLICATION.** Reports of completed research or a major significant phase of research that present the results of NASA programs and include extensive data or theoretical analysis. Includes compilations of significant scientific and technical data and information deemed to be of continuing reference value. NASA's counterpart of peer-reviewed formal professional papers but has less stringent limitations on manuscript length and extent of graphic presentations.
- **TECHNICAL MEMORANDUM.** Scientific and technical findings that are preliminary or of specialized interest, e.g., quick release reports, working papers, and bibliographies that contain minimal annotation. Does not contain extensive analysis.
- **CONTRACTOR REPORT.** Scientific and technical findings by NASA-sponsored contractors and grantees.

- **CONFERENCE PUBLICATION.** Collected papers from scientific and technical conferences, symposia, seminars, or other meetings sponsored or cosponsored by NASA.
- **SPECIAL PUBLICATION.** Scientific, technical, or historical information from NASA programs, projects, and mission, often concerned with subjects having substantial public interest.
- **TECHNICAL TRANSLATION.** English-language translations of foreign scientific and technical material pertinent to NASA's mission.

Specialized services that complement the STI Program Office's diverse offerings include creating custom thesauri, building customized databases, organizing and publishing research results...even providing videos.

For more information about the NASA STI Program Office, see the following:

- Access the NASA STI Program Home Page at <http://www.sti.nasa.gov>
- E-mail your question via the Internet to [help@sti.nasa.gov](mailto:help@sti.nasa.gov)
- Fax your question to the NASA Access Help Desk at 301-621-0134
- Telephone the NASA Access Help Desk at 301-621-0390
- Write to:  
NASA Access Help Desk  
NASA Center for AeroSpace Information  
7121 Standard Drive  
Hanover, MD 21076-1320  
301-621-0390

NASA/TM—2005–213609



# **Safe Affordable Fission Engine- (SAFE-) 100a Heat Exchanger Thermal and Structural Analysis**

*B.E. Steeve*

*Marshall Space Flight Center, Marshall Space Flight Center, Alabama*

National Aeronautics and  
Space Administration

Marshall Space Flight Center • MSFC, Alabama 35812

---

**March 2005**

Available from:

NASA Center for AeroSpace Information  
7121 Standard Drive  
Hanover, MD 21076-1320  
301-621-0390

National Technical Information Service  
5285 Port Royal Road  
Springfield, VA 22161  
703-487-4650

## TABLE OF CONTENTS

1. INTRODUCTION .....	1
2. STRUCTURAL DESIGN SUMMARY .....	2
3. DESIGN AND ANALYSIS HISTORY .....	3
4. METHODOLOGY .....	5
5. TEST CONDITIONS .....	6
6. DESIGN CRITERIA .....	7
6.1 Load Controlled Stress (NH-3222) .....	7
6.2 Inelastic Strains (T-1310) .....	8
6.3 Creep-Fatigue Damage (T-1411) .....	8
6.4 Weldments .....	9
7. FINITE ELEMENT MODEL .....	10
8. DIMENSIONS AND GEOMETRY .....	11
9. MATERIAL PROPERTIES .....	12
10. TEMPERATURE .....	13
11. LOADS .....	15
12. POSTPROCESSING .....	16
12.1 Sleeve-Weld Interface Axial Force and Moment .....	16
12.2 Section Stress at Critical Locations .....	16
12.3 Section Strain at Critical Locations .....	16
12.4 Creep-Fatigue Damage at a Point .....	17
13. RESULTS .....	19
13.1 Thermal Analysis Results .....	19
13.2 Heat Pipe Core Fixity .....	20
13.3 Pressure Only .....	20

## TABLE OF CONTENTS (Continued)

13.4 Thermal Stress Results .....	22
13.5 Welds .....	25
13.6 Braze Strength Effect .....	26
14. CONCLUSIONS .....	27
14.1 Braze Structural Requirement .....	27
APPENDIX A—MATERIAL PROPERTIES .....	29
APPENDIX B—PROOF TEST RESULTS .....	31
REFERENCES .....	37

## LIST OF FIGURES

1.	Solid model of SAFE-100a HX .....	1
2.	Cross section of an HX .....	2
3.	Ritz-Toast HX design finite element model .....	3
4.	Ritz-Toast high bending von Mises stress (psi) .....	4
5.	Octo-Block HX design concept finite element model .....	4
6.	Creep-fatigue damage envelope for 316 SS .....	9
7.	Finite element model .....	10
8.	Method of estimating linear distribution through wall thickness .....	17
9.	Temperature profile (°F) for brazed, 52-Btu/s, nonfailed heat pipe condition .....	19
10.	Temperature profile (°F) for brazed, 52-Btu/s, failed heat pipe condition .....	19
11.	Stress intensity (psi) due to pressure only—He, 52 Btu/s.....	21
12.	Maximum strain levels for each test condition .....	22
13.	Center sleeve axial stress versus cover plate thickness—brazed, 62-Btu/s, failed heat pipe .....	23
14.	Strain through center sleeve—brazed, 62-Btu/s, failed heat pipe .....	24
15.	Maximum creep-fatigue damage ratio .....	24
16.	Equivalent strain, brazed, 62-Btu/s, failed heat pipe .....	25
17.	SAFE-100a HX proof test setup .....	32
18.	Braze cup side .....	32
19.	Side opposite braze cups .....	33
20.	Barrel section .....	33

**LIST OF FIGURES (Continued)**

21.	Strains and pressure versus time .....	34
22.	Finite element model radial strain .....	34
23.	Comparison of test and predicted strain .....	35

## LIST OF TABLES

1.	Test conditions .....	6
2.	Braze properties .....	12
3.	Manifold and plenum thermal boundary conditions .....	13
4.	Heat pipe vapor temperatures .....	14
5.	Expected test cycle and life usage .....	18
6.	Heat pipe axial forces for a fixed core—brazed, 52 Btu/s .....	20
7.	Load-controlled stress results .....	21
8.	Maximum first principal strains and margins .....	23
9.	Weld factors of safety .....	25
10.	Effect of braze strength .....	26
11.	316L SS temperature-dependent material properties .....	29
12.	316L SS bilinear stress-strain curve data .....	29
13.	He-equivalent thermal conductivity .....	30
14.	Radiation gap equivalent thermal conductivity .....	30

## LIST OF ACRONYMS AND SYMBOLS

Ag	silver
ASME	American Society of Mechanical Engineers
BKIN	bilinear kenamatic hardening
Cu	copper
He	helium
HX	heat exchanger
LANL	Los Alamos National Laboratory
MPM	Material Properties Manual
MSFC	Marshall Space Flight Center
PVBC	Pressure Vessel and Boiler Code
SAFE	Safe Affordable Fission Engine
SS	stainless steel
TIG	tungsten inert gas
TM	Technical Memorandum

## NOMENCLATURE

$C$	constant (0.24)
$D$	damage
$Ftu_{\text{design}}$	ultimate tensile strength under design conditions
$Ftu_{\text{test}}$	ultimate tensile strength under test conditions
$i$	time point
$J$	sum of principle stresses
$j$	cycle type
$K$	section factor
$k$	time interval
$K_t$	$(K+1)/2$
$n$	number of applied cycles for cycle-type $j$
$N_d$	number of allowable cycles for cycle-type $j$
$o$	time point
$P$	total number of strain ranges
$P_b$	primary bending stress
$P_L$	local membrane stress
$P_m$	general primary membrane stress
$q$	total number of creep intervals
$R$	ratio of the weld metal creep rupture strength to the base metal creep-rupture strength
$S$	square root of the sum of the square of the principle stresses
$S_{\text{bend}}$	bending stress

## NOMENCLATURE (Continued)

$S_e$	equivalent stress
$S_{eqv}$	von Mises stress
$S_m$	time independent allowable stress
$S_{m+b}$	combined stress
$S_{memb}$	membrane stress
$S_{mt}$	the lower of $S_m$ and $S_t$
$S_r$	stress-to-rupture strength
$S_t$	time-dependent allowable stress
$t$	thickness
$T_d$	allowable creep time duration
$U_Z$	axial direction
$U_\Theta$	symmetry boundary
$\Delta_t$	duration of time interval $k$
$\epsilon_{eqv}$	equivalent tensile strain
$\epsilon_{xi}$	strain in the $x$ direction at time $i$
$\epsilon_{yo}$	strain in the $y$ direction at time $o$
$\epsilon_{yi}$	strain in the $y$ direction at time $i$
$\epsilon_{yo}$	strain in the $y$ direction at time $o$
$\epsilon_{zi}$	strain in the $z$ direction at time $i$
$\gamma_{xyi}$	shear strain in the $xy$ direction at time $i$
$\gamma_{yzi}$	shear strain in the $yz$ direction at time $i$
$\gamma_{zxi}$	shear strain in the $zx$ direction at time $i$
$\nu$	Poisson's ratio

## TECHNICAL MEMORANDUM

### SAFE AFFORDABLE FISSION ENGINE- (SAFE-) 100A HEAT EXCHANGER THERMAL AND STRUCTURAL ANALYSIS

#### 1. INTRODUCTION

The Safe Affordable Fission Engine- (SAFE-) 100a experiment is a thermal simulation of an in-space nuclear reactor core. The heat created by the nuclear fission process is simulated by electric heaters placed in the core fuel pins where the uranium would normally be. The heat from the core is transported out of the core via sodium-filled heat pipes that extend out of the core on one side. The heat pipes pass through a heat exchanger (HX) that extracts heat from the pipes and transfers it into a helium- (He-) argon gas mixture. This heated gas would then be used to drive an electric generator.

The HX is a welded stainless steel (SS) structure designed by Los Alamos National Laboratory (LANL). The structure is an annular flow design, where the bulk of the heat transfer occurs in the gas flowing through an annular passage around each heat pipe. The HX is designed to fit a core with nineteen heat pipes and sized to operate at the conditions needed for a Brayton cycle power conversion system. For the tests, the HX gas is passed through the test facility gas conditioning system. A full SAFE-100 reactor core consists of 61 heat pipe modules sized to generate 95 Btu/s of thermal power. Due to cost restraints, this experiment setup only uses the inner 19 modules and is called SAFE-100a. This Technical Memorandum (TM) describes the structural analysis and results of the SAFE-100a HX for several test conditions.

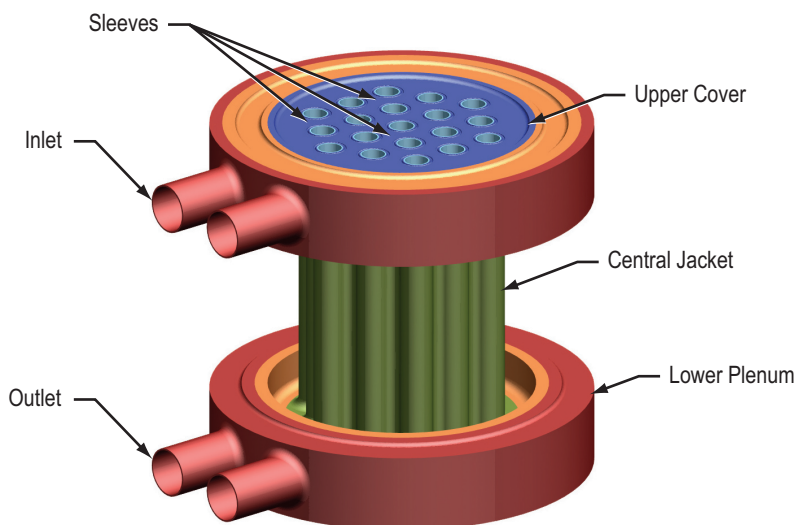


Figure 1. Solid model of SAFE-100a HX.

## 2. STRUCTURAL DESIGN SUMMARY

The HX (fig. 2) is fabricated from 316L SS and consists of 19 sleeves, an upper and lower cover, an upper and lower inner plenum, an upper and lower outer plenum, and a central jacket. All of the pieces are welded together by tungsten inert gas (TIG) or electron beam welding. During the manufacturing process, the HX will undergo several intermediate and a final annealing processes.

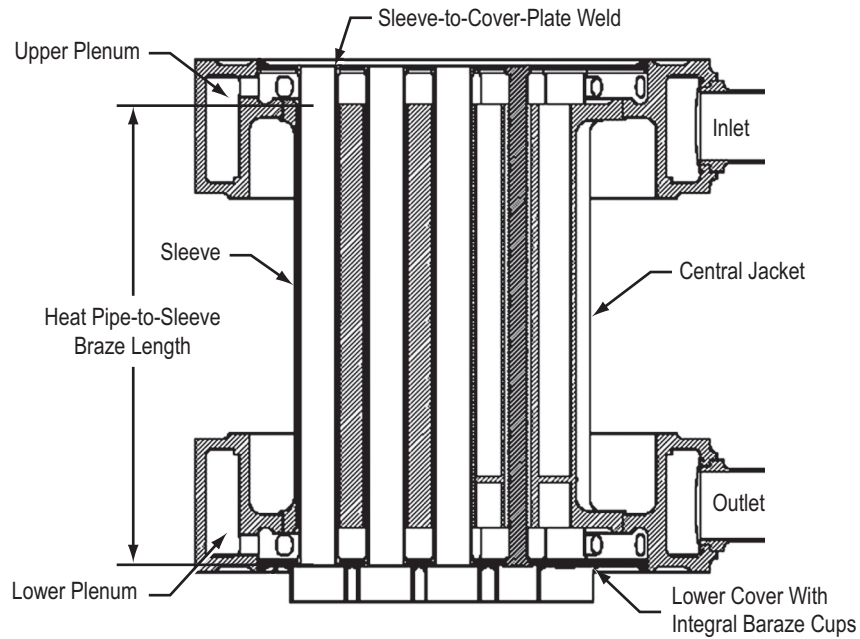


Figure 2. Cross section of an HX.

### 3. DESIGN AND ANALYSIS HISTORY

The original HX design concepts were numerous and varied. The first to be seriously pursued and analyzed was termed the Ritz-Toast design (figs. 3 and 4). This design had individual cross-flow HXs around separate rows of heat pipes. To fit an HX around each row, right next to each other, the design had to be thin. This created a flat pressure vessel that introduced high bending stresses in the flat wall around internal supports and was determined to be unacceptable and without any good design solutions.

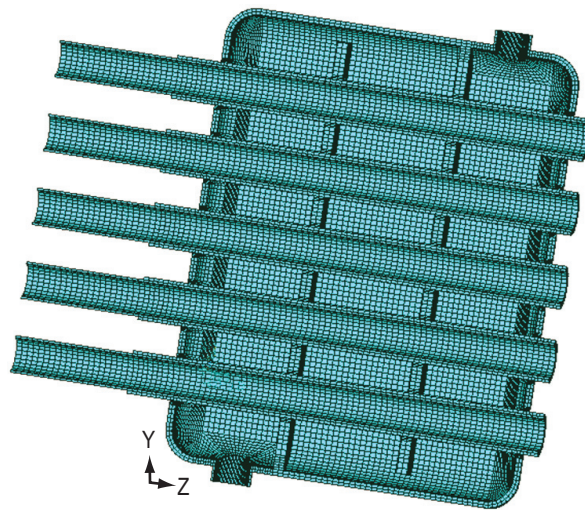


Figure 3. Ritz-Toast HX design finite element model.

The next design concept investigated was termed the Octo-Block design (fig. 5). This design also had individual HXs around each row of heat pipes but was an annular flow design with an inlet and outlet manifold. Since the pressure walls were cylinders, the pressure stresses were not a problem. However, this design was dropped due to heat transfer, flow, and plumbing issues.

The next design that made it to the analysis stage looked similar to the current design. It had the same flow design, but instead of a solid jacket section, it had individual jackets surrounding each sleeve for each heat pipe. For manufacturing ease and improved thermal conduction between the annular flow passages, the jackets were replaced in the current design as a solid piece with through holes to form the annular passages and blind holes to lighten the structure.

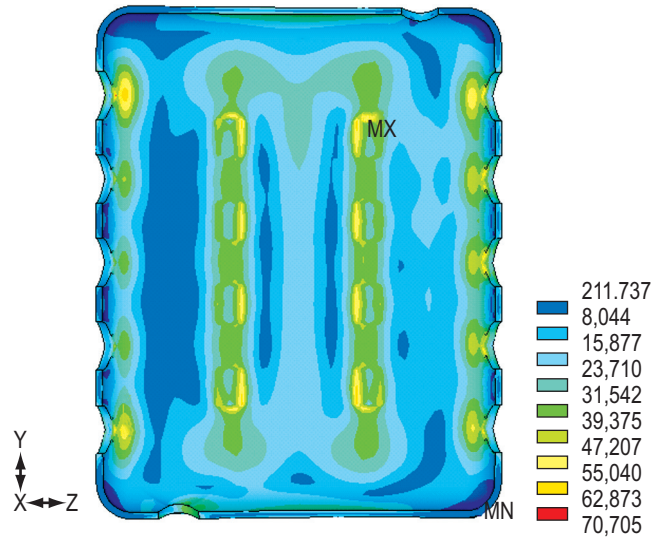


Figure 4. Ritz-Toast high bending von Mises stress (psi).

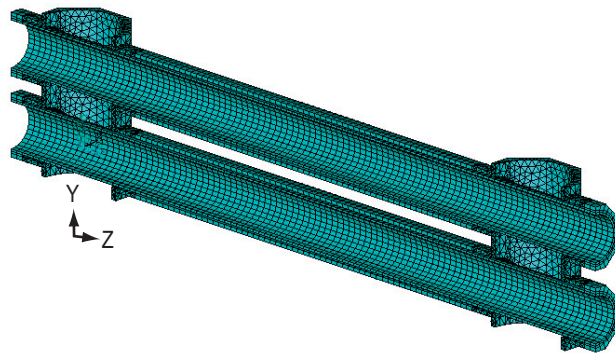


Figure 5. Octo-Block HX design concept finite element model.

#### **4. METHODOLOGY**

The HX analysis was performed using a finite element model of the HX along with the heat pipes and a small representation of the core. This model was used to solve for the temperature profile, which was then used in a structural solution. Only the steady state thermal condition was considered. The transient thermal heat up and cool down are assumed to be slow and less severe than the steady state condition. Hand calculations were used to evaluate the welds and pipe stub.

## 5. TEST CONDITIONS

There are 12 test conditions proposed for the SAFE-100a experiment with the HX. All 12 conditions will be analyzed. Table 1 lists the 12 conditions. Since the SAFE-100a experiment only has 19 pins (or modules) versus the full suite of 61 pins, it operates at 19/61 percent of full power. Table 1 lists the power level for both configurations. This TM refers to both the 19- and 61-pin power levels interchangeably.

Table 1. Test conditions.

Test No.	Gap Fill	Failed Heat Pipe	Power (Btu/s)		Flow (lbm/s)	Temperature (°F)		Pressure In (psi)
			19 Pin	61 Pin		In	Out	
H1	He	no	8.1	26	0.324	909	1,071	200
H2	He	no	16.2	52	0.324	621	947	200
H3	He	no	19.3	62	0.324	621	947	200
H4	He	yes	8.1	26	0.324	909	1,071	200
H5	He	yes	16.2	52	0.324	621	947	200
H6	He	yes	19.3	62	0.324	621	947	200
B1	braze	no	8.1	26	0.324	909	1,071	200
B2	braze	no	16.2	52	0.324	745	1,071	200
B3	braze	no	19.3	62	0.324	745	1,071	200
B4	braze	yes	8.1	26	0.324	909	1,071	200
B5	braze	yes	16.2	52	0.324	745	1,071	200
B6	braze	yes	19.3	62	0.324	745	1,071	200

The first six tests will be performed without any physical contact between the HX and the heat pipes. The test chamber will be filled with He to provide a medium to help transfer heat to the HX. The final six tests will be performed after brazing the HX to the heat pipes. The braze will provide the thermal path, and the test chamber will be pumped down to a vacuum.

Both the He and brazed cases will be performed with and without a failed heat pipe. For the cases without a failed heat pipe, all 19 heat pipes will be filled and work to transport the heat from the core to the HX. For the failed heat pipe cases, the center heat pipe will be replaced with an empty pipe. This pipe will, therefore, only conduct heat through its metal wall. The cases will be performed at three different power levels. In all cases the pressure will remain the same.

## 6. DESIGN CRITERIA

The HX operates at temperatures that range from 620 to 1,250 °F. At these temperatures, creep-induced failure of the structure is a possibility. There are two basic failure modes identified for the HX. They are an overpressure-induced failure of the pressure wall and creep-fatigue damage-induced cracking. To address these failure modes from an analysis and design standpoint, the criteria found in “ASME Pressure Vessel and Boiler Code”, section III: subsection NH was partially adopted for use.<sup>1</sup> Only portions of the code were used in the design and analysis of the HX. A summary of the criteria used is listed here. The code should be referred to for a complete explanation of the criteria.

For the purpose of this analysis, the pressure-induced stress is considered to be the primary stress, and the thermal induced stresses are considered to be secondary stresses. The thermal stress is only considered in the strain and creep-fatigue damage criteria.

### 6.1 Load Controlled Stress (NH-3222)

Only the level A and B service limits are considered in this analysis. The design and level C and D limits are not used. The level A and B service limits are

$$P_m \leq S_{mt} \quad , \quad (1)$$

$$P_L + P_b \leq K \cdot S_m \quad , \quad (2)$$

and

$$P_L + \frac{P_b}{K_t} \leq S_t \quad , \quad (3)$$

where

- $P_m$  = general primary membrane stress
- $P_L$  = local primary membrane stress
- $P_b$  = primary bending stress
- $S_m$  = time-independent allowable stress
- $S_t$  = time dependent allowable stress
- $S_{mt}$  = lower of  $S_m$  and  $S_t$
- $K$  = section factor (1.5 for a rectangular section)
- $K_t$  =  $(K+1)/2$ .

## 6.2 Inelastic Strains (T-1310)

The inelastic strains should not exceed the following for the maximum principal strain:

- One percent averaged through the thickness.
- Two percent due to a linear distribution of strain through the thickness.
- Five percent at any point.

## 6.3 Creep-Fatigue Damage (T-1411)

Fatigue is evaluated using a local equivalent strain range and compared to the fatigue allowable given in appendix T of subsection NH:<sup>1</sup>

$$\Delta \varepsilon_{eqv,i} = \frac{\sqrt{2}}{2(1+\nu)} \left[ (\Delta \varepsilon_{xi} - \Delta \varepsilon_{yi})^2 + (\Delta \varepsilon_{yi} - \Delta \varepsilon_{zi})^2 + (\Delta \varepsilon_{zi} - \Delta \varepsilon_{xi})^2 + \frac{3}{2} (\Delta \gamma_{xyi}^2 + \Delta \gamma_{yz i}^2 + \Delta \gamma_{zxi}^2) \right]^{\frac{1}{2}} . \quad (4)$$

The change in the strain components between time  $i$  and time  $o$ , where time  $o$  is at an extreme minimum or maximum, is given by

$$\Delta \varepsilon_{yi} = \varepsilon_{yi} - \varepsilon_{yo} , \quad (5)$$

and so forth. The term  $\nu$  is 0.5.

The combined creep and fatigue damage allowable is given by the relation

$$\sum_{j=1}^P \left( \frac{n}{N_d} \right)_j + \sum_{k=1}^q \left( \frac{\Delta t}{T_d} \right)_k \leq D , \quad (6)$$

where

first term	= fatigue ratio
second term	= creep ratio
$n$	= number of applied cycles for cycle type $j$
$N_d$	= number of allowable cycles for cycle type $j$
$\Delta t$	= duration of the time interval $k$
$T_d$	= allowable time duration for time interval $k$ .

The total damage,  $D$ , should not exceed the creep-fatigue damage specified in reference 1 for 316 SS and shown in figure 6.

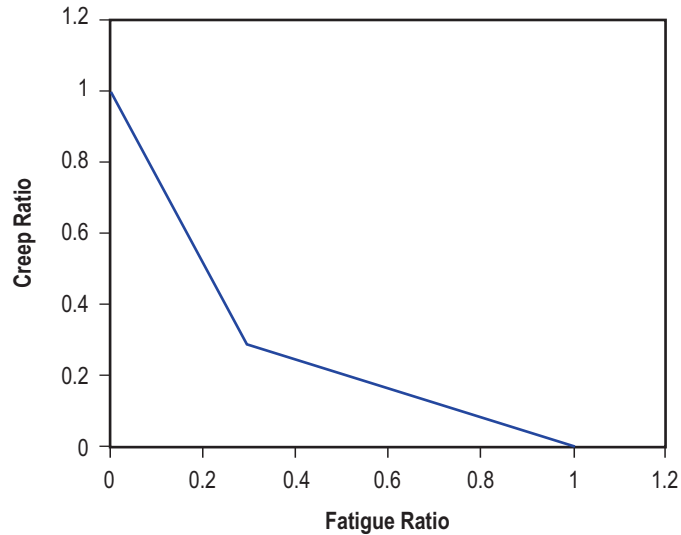


Figure 6. Creep-fatigue damage envelope for 316 SS.<sup>1</sup>

#### 6.4 Weldments

For regions within the heat-affected zone of a weld, the strength and life allowables are modified per the following:

- Load controlled stress:
  - The allowable limits for  $S_t$  and  $S_{mt}$  are the lower of  $S_t$  or  $S_{mt}$  and  $0.8 \times S_r \times R$ .
  - The stress-to-rupture strength value for a given time and temperature is  $S_r$ . The ratio of the weld metal creep rupture strength to the base metal creep rupture strength is  $R$ , as found in table I–14.10B of the ASME Pressure Vessel and Boiler Code (PVBC).<sup>1</sup>
- Inelastic strains: The strain limits for a welded region are one half of the allowable for the base material.
- Creep-fatigue damage:
  - The number of allowable cycles for low cycle fatigue is one half of the number allowed for the base metal.
  - The allowable time duration is determined from a stress-to-rupture curve by multiplying the base material stress-to-rupture values by the ratio,  $R$ .

## 7. FINITE ELEMENT MODEL

The arrangement of the heat pipe modules in the core repeats every  $60^\circ$ , and each of these sections is symmetric about its axial midplane. The thermal profile is assumed to not vary in the circumferential direction. Therefore, a  $30^\circ$  or  $1/12$ th section with symmetry boundary conditions is sufficient to model the behavior of the entire HX. The finite element model (fig. 7) of the HX, then, is a  $1/12$ th symmetry representation of the HX, heat pipes, and partial core. The model is built and solved using ANSYS 7.0 and is meshed with tetrahedron (SOLID186) and quad brick (SOLID185) elements. Transitional pyramid-shaped elements are used between the interface of the tetrahedron and quad elements. The model geometry was built from scratch using the geometry and dimensions from a solid model created and provided by LANL.

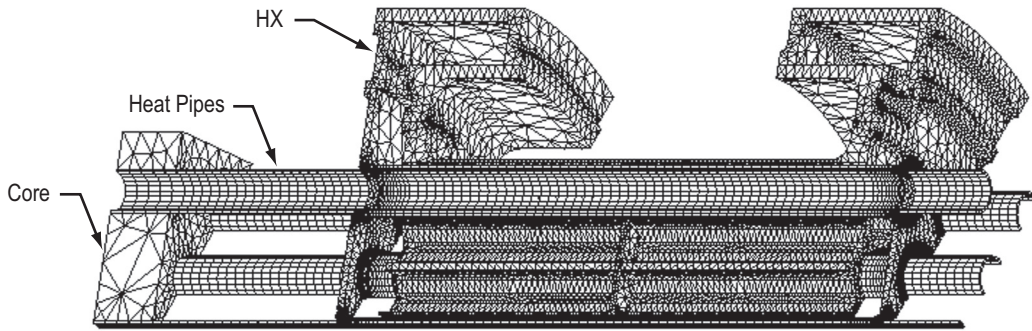


Figure 7. Finite element model.

Symmetry boundary conditions,  $U_\theta=0$ , are placed on the axial symmetry planes. The axial direction is restrained,  $U_z=0$ , on the bottom of the core and the bottom of the outlet manifold at the outer edges. For the He cases, the heat pipes are coupled to the core in all directions. For the braze conditions, the heat pipes are coupled to the core only in the radial and circumferential directions with the heat pipes free to slide through the core in the axial direction. The thermal and structural loads were applied to the appropriate surfaces of the model as described in section 10. The material properties used in the model are described in section 11.

## **8. DIMENSIONS AND GEOMETRY**

The dimensions and geometry for the finite element model were taken from a solid model created by LANL. To reduce the element count, small features, such as chamfers and very skinny areas, were not included in the finite element model. Except for the inlet and outlet pipes, all significant structural features are included. Nominal dimensions are used in the finite element model.

The orientation of the HX with respect to the core is with the inlet away from the core. This orientation places the hot outlet side of the HX closer to the core to help minimize the radial thermal growth mismatch between the core and the HX. The HX is located a distance of 8 cm away from the core.

The heat pipes are all centered within the HX sleeves. For the brazed test conditions, a solid braze from the outer edge of the outlet cover plate to the plane of the solid jacket core on the inlet side is assumed.

## 9. MATERIAL PROPERTIES

The HX is constructed from 316L SS. The various pieces are then welded together by either the electron beam or TIG process. The HX will undergo several annealing processes as well as a braze cycle. Therefore, the 316L SS properties are for the annealed condition. The plastic behavior of the HX was treated as a bilinear stress-strain curve in the model. The ANSYS bilinear kinematic hardening (BKIN) material model was used to represent this inelastic behavior. All material properties were taken from the Rocketdyne “Material Properties Manual” (MPM), sections 2211 and 2212, and MIL-HDBK-5F.<sup>2,3</sup> Appendix A of this TM lists the properties used in this analysis.

For the brazed cases, the HX is brazed to the heat pipes using the silver- (Ag-) based braze alloy Nicusil-8 (BAg-13a). Its composition is Ag 56:copper (Cu) 42:nickel (Ni) 2, and it has a solidus of 1,417 °F and a liquidus of 1,638 °F. There are no readily available properties for this braze at elevated temperatures. An attempt was made to pull together some properties for use in the finite element model based on very limited braze properties and a review of Ag and Cu properties at elevated temperatures. Table 2 lists the properties that were used. These properties are guesses and not verified. One of the guidelines in coming up with these properties was to make the braze soft and weak compared to SS.

Table 2. Braze properties.

Nicusil-8 Braze Properties					
Property	Units	70 °F	800 °F	1,000 °F	1,200 °F
Thermal conductivity	Btu/hr-ft-°F	136	112	110	108
	W/m-K	235	194	190	187
Coefficient of thermal expansion	in/in/°F	8.4	10	11	12
	m/m/K	15.1	18	19.8	21.6
Elastic modulus	msi	14	12	11	10
	GPa	97	83	76	69
Poisson's ratio	–	0.35	0.35	0.35	0.35
Yield strength	ksi	25	12	10	8
	MPa	172	83	69	55
Tangent modulus	ksi	100	80	80	80
	MPa	689	552	552	552

## 10. TEMPERATURE

Being an HX, the temperature varies throughout the component. These temperature gradients create thermal loads and strains that dominate the structural performance. The temperature profile used in the analysis is generated by applying thermal boundary conditions to the finite element model and then solving for the steady state thermal solution.

The thermal conditions for the annular flow between the HX sleeve and jacket were calculated and provided by LANL. The heat transfer coefficient for the sleeve and jacket and the temperature of the heat pipe and coolant were provided as a function of position down the length of each row of annular flow paths. Failed heat pipe conditions were provided for the center failed heat pipe annulus and the adjacent coolant paths. The thermal conditions for the outer two rows are assumed to remain the same for both the nonfailed and failed heat pipe conditions. The thermal conditions for the inner and outer manifold regions of both the inlet and outlet were calculated by the Structures, Mechanics, and Thermal Department (ED25) of Marshall Space Flight Center (MSFC). Table 3 lists the results of these calculations.<sup>4</sup>

Table 3. Manifold and plenum thermal boundary conditions.

Fluid Temperature (°F)		Flow Rate (lbm/s)	Heat Transfer Coefficient (Btu/ft <sup>2</sup> -hr-°F)			
			Inlet		Outlet	
Inlet	Outlet		Manifold	Plenum	Manifold	Plenum
621	947	0.324	1,102	1,590	1,136	1,374
621	947	0.324	1,261	1,817	1,295	1,573
745	1,071	0.324	1,130	1,670	1,158	1,431
745	1,071	0.324	1,283	1,891	1,312	1,618
909	1,071	0.324	1,130	1,624	1,147	1,528

The lightening holes in the solid jacket are assumed to be adiabatic and have no thermal boundary conditions on any of these surfaces. The exterior of the HX was also assumed to be adiabatic.

For the He test conditions, an equivalent thermal conductivity was used for the elements between the heat pipe and the HX sleeves in the thermal runs. For the brazed test conditions, an equivalent thermal conductivity was used for the elements in the vacuum gap between the heat pipe and the HX sleeves in the unbrazed region. These equivalent conductivities are listed in appendix A.

The axial temperature profiles of the heat pipes were specified by LANL for both the annular flow region and the length between the HX and core. These temperatures were applied to the inner diameter of the heat pipes. The core was allowed to conduct to a steady state solution based on the temperature specified for the heat pipes. The temperatures for the heat pipes between the core and HX (heat pipe vapor temperature) are given in table 4.

Table 4. Heat pipe vapor temperatures.

Test Condition				Heat Pipe Vapor Temperature (°F)			
Test No.	Gap Fill	Failed Heat Pipe	Power (Btu/s)	Center	Ring 1	Ring 2 Mid-side	Ring 2 Corner
H1	He	no	8.1	1,156	1,147	1,139	1,131
H2	He	no	16.2	1,124	1,107	1,090	1,074
H3	He	no	19.3	1,157	1,137	1,118	1,099
H4	He	yes	8.1	failed	1,170	1,139	1,131
H5	He	yes	16.2	failed	1,153	1,090	1,074
H6	He	yes	19.3	failed	1,176	1,118	1,099
B1	braze	no	8.1	1,097	1,094	1,090	1,105
B2	braze	no	16.2	1,125	1,117	1,110	1,104
B3	braze	no	19.3	1,132	1,124	1,116	1,109
B4	braze	yes	8.1	failed	1,135	1,090	1,105
B5	braze	yes	16.2	failed	1,201	1,110	1,104
B6	braze	yes	19.3	failed	1,210	1,116	1,109

## **11. LOADS**

The pressure for each load case is 200 psi (1.38 MPa) and is applied to all of the interior surfaces. There are no other loads applied to the model.

## 12. POSTPROCESSING

Several postprocessing techniques are employed to extract relevant data from each of the finite element solutions. Sections 12.1–12.4 describe each of these methods.

### 12.1 Sleeve-Weld Interface Axial Force and Moment

The axial force and moment about the global circumferential axis is determined using an ANSYS macro. This macro selects the nodes on the sleeve-to-upper-cover interface and then sums the force at each node in the axial direction to obtain the total axial force. The contribution of each nodal force to the moment about the global circumferential axis is also summed based on the force and the distance from the axis. This macro also determines the total axial force at the upper cover-to-outer-manifold interface. The results are then sent to an output file.

### 12.2 Section Stress at Critical Locations

The ASME PVBC design criteria are based on membrane and bending stress intensity across a section. To get these stresses, an ANSYS macro is used to compute the membrane and bending stress through several critical locations. These critical sections are the peak stress intensity location on the outside of each sleeve, the peak stress intensity location on the inside and outside of both the inlet and outlet covers, the peak stress intensity location on the outside of the side wall of the outer manifold, and the peak stress intensity location on the inside of the through holes of the jacket.

A path is created at each critical location from the peak stress intensity surface node to a node closest to a point on the opposite surface of the wall normal to the wall surface. The section stress command within ANSYS is used to compute the membrane and bending component stress for each of the paths. The membrane and bending stress intensity is then computed from the section component membrane stresses. The membrane and bending stress components are combined according to  $S_{m+b} = S_{memb} + S_{bend} / 1.25$  per the ASME PVBC criteria found in NH-3223.<sup>1</sup> These combined component stresses are then used to compute the membrane plus bending stress intensity.

### 12.3 Section Strain at Critical Locations

The allowable strains for any section are listed in the ASME PVBC, appendix T-1310.<sup>1</sup> They are the average, linearized surface, and maximum point strain based on the maximum positive principal strain. To obtain these values, an ANSYS macro is used. This macro creates a path at critical locations as described in section 12.2. The critical locations evaluated are the peak first principal strain location of the outside of each sleeve and the peak first principal strain location of the inside and outside of the inlet and outlet covers.

To calculate the average strain, the component strains are determined along each path. The component strains at each path point are then averaged and used to determine the average first principal strain. The strain at the surface, based on a linearized strain profile, is estimated using the first principal strain profile along the path. This is done according to figure 8.

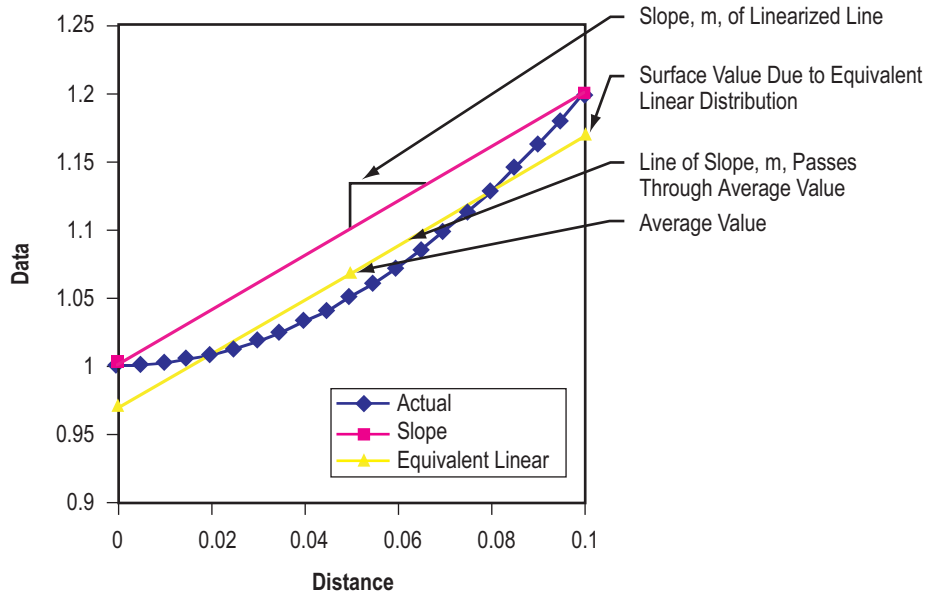


Figure 8. Method of estimating linear distribution through wall thickness.

## 12.4 Creep-Fatigue Damage at a Point

The strain and stress at critical locations are extracted by a macro for use with the creep-fatigue damage criteria. The macro finds the maximum strain (total equivalent strain), stress (von Mises stress), and temperature location of each sleeve, inlet cover, and outlet cover. The total equivalent strain at each of these points is extracted to compare with the low cycle fatigue allowable. This analysis uses the total equivalent strain at the steady state thermal condition as the total strain range to enter the low cycle fatigue curve.

An equivalent stress at each point is calculated according to  $S_e = S_{eqv} \times \exp(C(J/S - 1))$  per the ASME PVBC in paragraph T-1411.<sup>1</sup> This stress is then used to find the allowable creep life from the stress-to-rupture curve.

In order to calculate a creep-fatigue damage ratio, an expected test usage was used (table 5). Using the strain and temperature at each critical point, an allowable number of cycles was determined from the low cycle fatigue curve per figure T-1420-1B of ASME PVBC.<sup>1</sup> Points between values on the curve were linearly interpolated. A fatigue damage ratio was then determined for each test condition.

Table 5. Expected test cycle and life usage.

Test No.	Gap Fill	Failed Heat Pipe	Power (Btu/s)	No. Cycles	Total Test Time (hr)
H1	He	no	8.1	14	40
H2	He	no	16.2	3	12
H3	He	no	19.3	3	12
H4	He	yes	8.1	5	16
H5	He	yes	16.2	3	12
H6	He	yes	19.3	3	12
B1	braze	no	8.1	14	40
B2	braze	no	16.2	3	12
B3	braze	no	19.3	3	12
B4	braze	yes	8.1	5	16
B5	braze	yes	16.2	3	12
B6	braze	yes	19.3	3	12

The equivalent stress,  $S_e$ , and temperature at each critical point were used to enter the stress-to-rupture table and determine an allowable creep life for each test condition, a life ratio was calculated, and the sum of all the fatigue ratios and life ratios for each component were computed.<sup>6</sup> These sums were then plotted against the allowable creep-fatigue damage curve.

## 13. RESULTS

### 13.1 Thermal Analysis Results

The steady state thermal solution was solved for each of the twelve test conditions using the thermal boundary conditions given for each case as described above. Figures 9 and 10 show the temperature profile for a brazed, 52-Btu/s, nonfailed heat pipe and failed heat pipe condition.

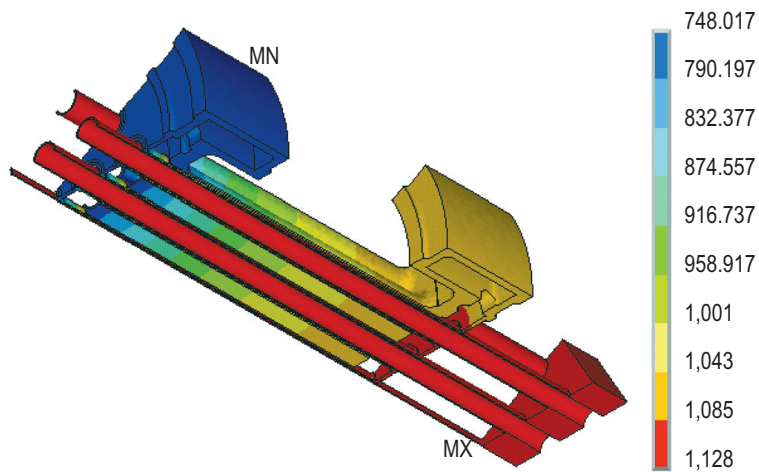


Figure 9. Temperature profile (°F) for brazed, 52-Btu/s, nonfailed heat pipe condition.

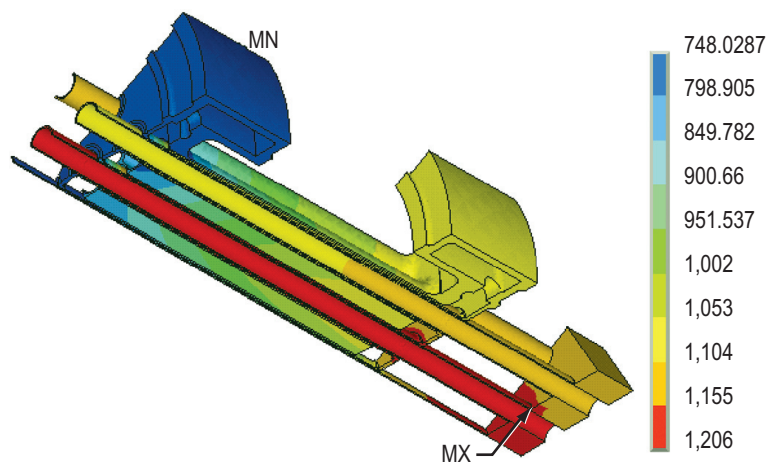


Figure 10. Temperature profile (°F) for brazed, 52-Btu/s, failed heat pipe condition.

### 13.2 Heat Pipe Core Fixity

One of the boundary conditions that was found to have a significant effect on the HX results was the assumed fixity of the heat pipes in the core. The heat pipes and core were initially one solid piece with either all or a portion of the core fixed in the axial direction. This essentially forces the axial displacement of the heat pipes to be zero at the core. This strongly effects the displacements at the HX outlet cover plate by not allowing the outlet cover plate to move axially due to the differences in thermal growth for each heat pipe/sleeve. The only way this boundary condition can occur in the current design of the core is for each heat pipe module to be kept from slipping due to friction and the compressive forces that develop in the core due to the radial restraints of the core.

It seems unlikely that the core would restrain a heat pipe module from slipping due to the differences in thermal growth. The magnitude of the forces that develop in the heat pipes with the heat pipes fixed axially were checked and are listed in table 6 for a brazed, 52-Btu/s condition. Assuming a friction factor of 0.5 between the SS heat pipe modules, a load of 1,200 lb would be required to prevent the module from slipping.

Table 6. Heat pipe axial forces for a fixed core—brazed, 52 Btu/s.

Heat Pipe	Axial Load (lb)
Center	537.6
Ring 1	-600.2
Ring 2 mid	275.2
Ring 2 corner	235.2

Releasing the heat pipes in the axial direction creates a more severe condition for the HX because that allows the outlet cover plate to displace according to the thermal growth of each heat pipe/sleeve. Since this is a more severe condition, the analysis of the HX includes the release of the heat pipes in the axial direction at the core. If testing or analysis of the core shows that the core prevents the modules from slipping, then this boundary condition can be revisited.

### 13.3 Pressure Only

In order to remove the thermal induced stress and strain, the pressure-only cases were run with the coefficient of thermal expansion set to zero . Since pressure in this case is the only load, the results for each test condition are about the same. The only difference is due to the change in the material properties (Young's modulus and Poisson's ratio) due to the temperature differences between the test conditions. The stress levels for the pressure-only cases were low enough to stay below the SS yield point, so the cases were run elastically.

Figure 11 is a plot of the stress intensity for the He 52-Btu/s condition. The maximum stress locations occur in the cover plates at the largest unsupported span. The peak stress is indicated at a point in the jacket wall. This peak is at one node and appears to be an artificial artifact of the model.

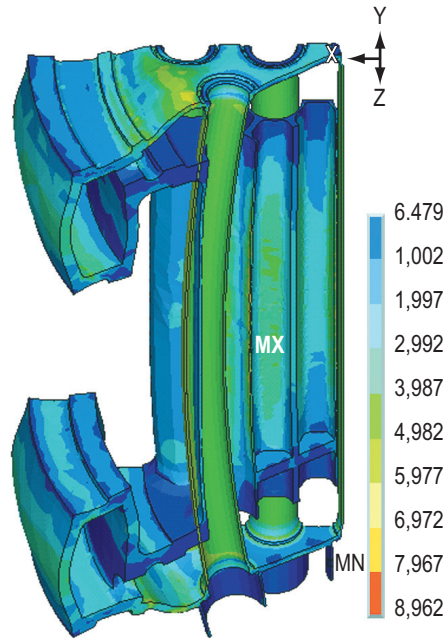


Figure 11. Stress intensity (psi) due to pressure only—He, 52 Btu/s.

The criteria for assessing the pressure-induced stresses are based on the membrane and bending stress through a section. Table 7 lists the membrane and bending stresses for the criteria through the wall thickness at the point of maximum stress intensity for the jacket and cover plates for each of the 52-Btu/s test conditions.

Table 7. Load-controlled stress results.

Test	Temperature (°F)	$P_m$ (psi)	$P_L+P_b$ (psi)	$P_L+P_b/K_t$ (psi)	Margin of Safety		$S_t$ Life (hr)
					$S_{mt}$	$S_m$	
Jacket							
H2	846	5,319	8,960	8,224	1.54	1.26	100,000
H5	861	5,322	8,967	8,230	1.54	1.26	100,000
B2	1,002	5,287	8,905	8,173	1.55	1.27	100,000
B5	1,014	5,290	8,913	8,180	1.5	1.26	100,000
Upper Cover							
H2	862	3,018	8,212	7,151	3.47	1.47	100,000
H5	863	3,020	8,223	7,160	3.47	1.46	100,000
B2	801	3,331	9,083	7,886	3.05	1.23	100,000
B5	801	3,332	9,091	7,892	3.05	1.23	100,000
Lower Cover							
H2	1,039	2,434	7,404	6,387	4.23	1.67	100,000
H5	1,044	2,444	7,429	6,409	4.16	1.65	100,000
B2	1,107	3,369	8,433	7,377	1.72	1.23	100,000
B5	1,107	3,369	8,434	7,378	1.72	1.23	100,000

The results listed in table 7 show that the HX has sufficient margin against pressure induced burst and stress-rupture failure.

### 13.3.1 Proof Test

The HX was proof tested before installation in the SAFE-100a experiment. The proof factor is 1.25, and an environmental correction factor was applied to account for the difference between the material strength at room temperature and the elevated test temperature. The environmental correction factor is  $70/43=1.63$  (316L strength at 70 °F/strength at 1,200 °F). The required proof pressure is  $200 \text{ psi} \times 1.25 \times 1.63 = 407 \text{ psi}$  minimum with the maximum proof pressure as 430 psi ( $420 \pm 10 \text{ psi}$ ). The proof-pressure case was run at 430 psi. The minimum margin of safety occurs in the upper cover and is 0.82. Appendix B includes the results of the actual proof test.

## 13.4 Thermal Stress Results

The temperature distribution within the HX develops internal thermal stresses and strains throughout the part. The failed heat pipe conditions are the most severe because the cold failed heat pipe is surrounded by hot active heat pipes. The stresses and strains for this condition are concentrated primarily around the sleeve-to-cover-plate joint. Figure 12 plots the maximum equivalent strain for the highest four strained parts for each test condition.

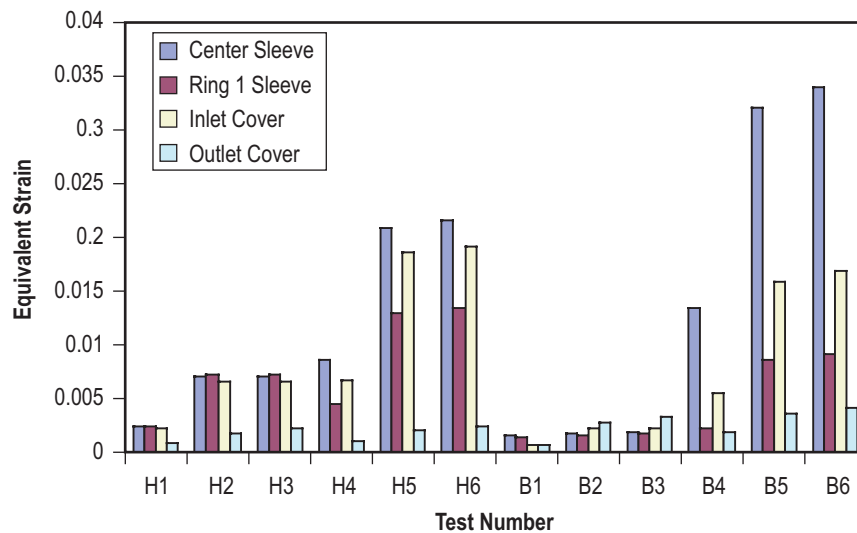


Figure 12. Maximum strain levels for each test condition.

### 13.4.1 Cover Plate Thickness

The cover plate thickness was found to have a significant effect on the structural behavior of the HX, and this effect is most pronounced for the failed heat pipe conditions. This is because the difference in axial thermal growth between the cool failed heat pipe/sleeve and hot adjacent heat pipes/sleeves

must be accommodated by the bending of the cover plates over a relatively small distance. Figure 13 plots the net section axial stress in the center sleeve versus cover thickness. A thickness of 0.1 in was chosen to keep the axial stress below the yield stress at the maximum center sleeve temperature.

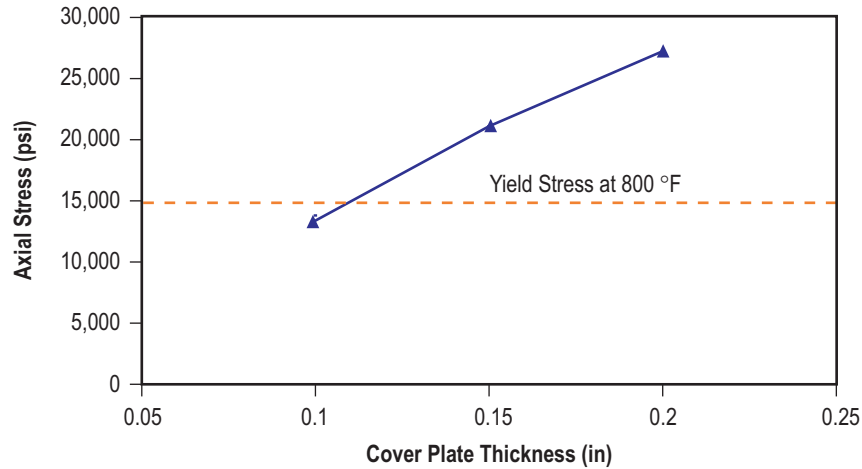


Figure 13. Center sleeve axial stress versus cover plate thickness—brazed, 62-Btu/s, failed heat pipe.

### 13.4.2 Inelastic Strain

The strain through the wall thickness of each component was evaluated using the automated process described in section 12.3. It is assumed that the peak strains occur in the heat-affected zone of the sleeve-to-cover-plate weld. Therefore, the weld allowables are used to compute the margins of safety. The minimum margins of safety against the ASME strain criteria are listed in table 8. The surface strain due to an equivalent strain distribution in the center sleeve exceeds the criteria by  $\approx 10$  percent in the brazed, 62-Btu/s test condition only. All other conditions have positive margins.

Table 8. Maximum first principal strains and margins.

Component	Test	$\epsilon_{avg}$	$\epsilon_{linear}$	$\epsilon_{max}$	MS <sub>avg</sub>	MS <sub>linear</sub>	MS <sub>max</sub>
Center sleeve	B6	0.0084	0.0211	0.0257	0.2	-0.1	0.9
Ring 1 sleeve	H6	0.0085	0.0113	0.013	0.2	0.8	2.8
Upper cover	H6	0.0048	0.0099	0.0119	0	0	1.1
Lower cover	B6	0.0009	0.0023	0.0027	4.6	3.3	8.3

Since the surface strain is estimated using the method shown in figure 8, the strain through the center sleeve that produced the negative margin was reevaluated using an actual linear curve fit. Figure 14 shows that a linear curve fit produces a surface strain of 1.96 percent, which corresponds to a margin of +0.02.

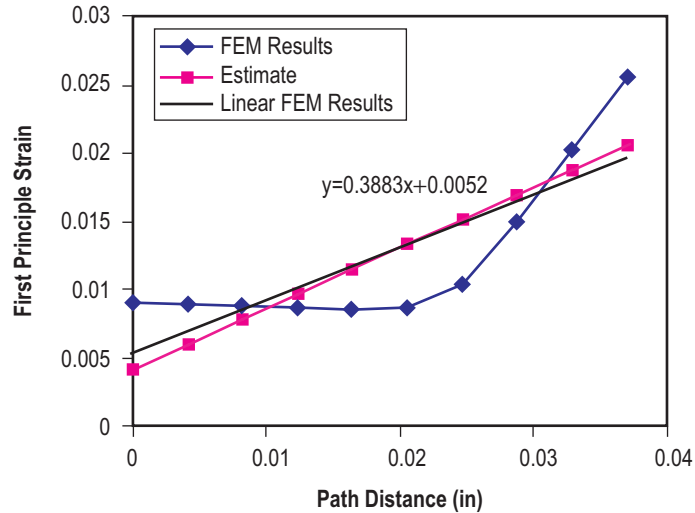


Figure 14. Strain through center sleeve—brazed, 62-Btu/s, failed heat pipe.

### 13.4.3 Creep-Fatigue

The creep-fatigue results were compiled using the automated routine described in section 12.4. The maximum calculated damage ratio for the four most severely loaded components is shown in figure 15. The center sleeve has the highest damage ratio at 1, primarily due to the magnitude of the strains that occur in the failed heat pipe conditions. These results assume that the peak strains all occur within the sleeve-to-cover-plate weld heat-affected zone, and therefore, the weld criteria is used to calculate the damage. If the nonweld criterion is used, then the damage fraction for the center sleeve drops to 0.5. Figure 16 shows the strain levels for the worst case and location of the maximum strain in the fillet of the center sleeve.

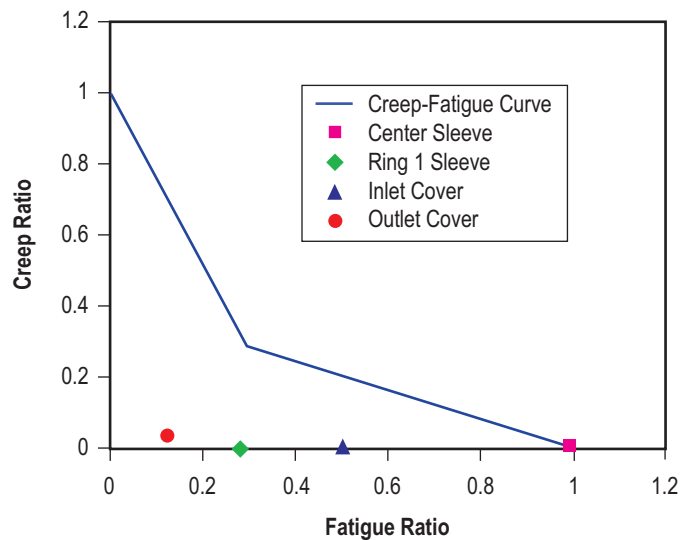


Figure 15. Maximum creep-fatigue damage ratio.

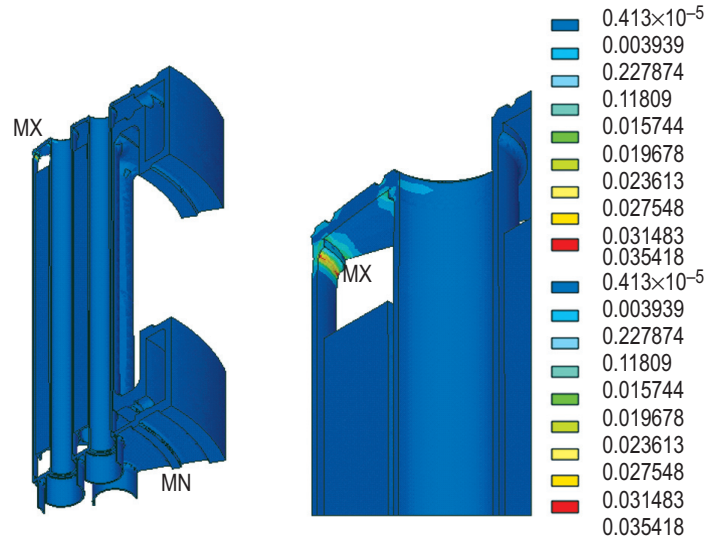


Figure 16. Equivalent strain, brazed, 62-Btu/s, failed heat pipe.

### 13.5 Welds

The welds in the HX were analyzed by hand. The loads for each weld were either extracted from the finite element model or calculated. Full penetration welds are assumed. The weld strength allowable used is 80 percent of the parent 316L material strength. Table 9 lists the calculated factors of safety for each weld.

Table 9. Weld factors of safety.

Weld	Factor of Safety
Sleeve to cover plate	4.4
Cover plate to inner plenum	19.1
Jacket to inner plenum	29.2
Inner plenum to outer ring	high
Pipe stub to plenum	3.5

The pipe stub-to-plenum weld factor of safety in table 9 is for the pressure load only on the external structural skip weld. Although there should not be a significant moment on the pipe stub since the coolant piping includes flex lines, the structural, skip-weld possesses less moment carrying capability than the pipe itself. If the internal seal weld is included, then the welds have more moment carrying capability than the pipe.

### 13.6 Braze Strength Effect

The effect of the heat pipe-to-braze strength on the behavior of the HX was evaluated. Two additional brazed, 62-Btu/s, failed heat pipe cases were run. In one, the braze material properties were set to be 316L SS, and the other case, the braze was completely removed. The thermal profile for each case was the same. The results were then compared with the standard case using the Nicusil-8 braze properties listed in table 2. Table 10 lists the results and the differences for some of the peak stress/strain locations.

Table 10. Effect of braze strength.

Analysis Result	Braze, 62-Btu/s, Failed Heat Pipe Results				
	Nicusil-8	SS 316L		Missing	
	Value	Value	% D	Value	% D
Center sleeve axial force (lb)	999	1,001	0.2	965	-3.4
Center sleeve maximum equivalent strain	0.0337	0.0339	0.6	0.0276	-18.1
Center sleeve maximum equivalent stress (psi)	29,340	29,419	0.3	27037	-7.8

Table 10 shows that there is little difference between the SS braze and the Nicusil-8 braze. The missing braze case is actually a less severe case. Since the heat pipes are hotter and expand more, removing the braze does not introduce as much thermal stress and strain into the HX.

## 14. CONCLUSIONS

The HX was evaluated for its expected pressure and thermal loads. Sufficient margin was found against the pressure load, even at the elevated temperatures. The thermal loads were found to be more severe, especially for the failed heat pipe conditions. Regions of plastic deformation occur due to the failed heat pipe loads around the sleeve-to-cover-plate welds. Running multiple tests with a failed heat pipe condition causes low cycle fatigue to be the primary failure mode of concern. The calculated damage ratio is at the maximum allowable of 1 for the proposed test series. The sleeve-to-cover-plate welds are, therefore, the most critical location in the HX design. It is important to develop the welding/inspection process of these welds to ensure high quality, void-free welds.

### 14.1 Braze Structural Requirement

Currently the maximum axial load that develops in the sleeves is 999 lb, which occurs in the failed heat pipe. The minimum sleeve area is 0.0748 in<sup>2</sup>. This results in an axial stress of 13,356 psi. The yield strength of 316L at 800 °F is 15 ksi. Based on these numbers and the results shown above, the braze is not essential to maintaining the structural integrity of the HX.

## APPENDIX A—MATERIAL PROPERTIES

Table 11. 316L SS temperature-dependent material properties.

Temperature (°F)	Thermal Conductivity (Btu/hr-ft-°F)	Density (lbm/ft <sup>3</sup> )	Specific Heat (Btu/lbm-°F)	Thermal Expansion (10 <sup>-6</sup> /R)	Young's Modulus (psi×10 <sup>6</sup> )	Poisson's Ratio	Yield Strength (ksi)	Ultimate Strength (ksi)
-400	5.43	504.4	0.063	5	29.2	0.285	50	184
-300	5.93	502.8	0.075	5.83	29.1	0.287	41	150
-200	6.43	501.3	0.085	6.55	28.9	0.29	36	120
-100	6.91	499.7	0.095	7.19	28.6	0.294	32	95
0	7.38	498.2	0.103	7.75	28.2	0.298	27	77
100	7.84	496.6	0.110	8.23	27.8	0.302	24	69
200	8.29	495.1	0.116	8.64	27.2	0.307	22	66
300	8.74	493.5	0.121	8.98	26.7	0.311	22	63
400	9.18	492	0.125	9.27	26	0.315	21	61
500	9.62	490.4	0.128	9.51	25.4	0.319	19	59
600	10.05	488.9	0.131	9.71	24.7	0.322	17	58
700	10.47	487.3	0.133	9.87	24	0.326	16	58
800	10.9	485.8	0.134	10.01	23.4	0.329	15	57
900	11.32	484.2	0.136	10.12	22.7	0.331	15	55
1,000	11.74	482.7	0.137	10.22	22	0.334	15	53
1,100	12.15	481.1	0.139	10.31	21.4	0.336	14	49
1,200	12.57	479.6	0.141	10.4	20.7	0.338	13	43
1,300	12.98	478.1	0.143	10.49	20.1	0.34	11	34
1,400	13.39	476.5	0.146	10.6	19.5	0.343	9	26
1,500	13.81	475	0.149	10.72	18.9	0.346	6	20
1,600	14.22	473.4	0.153	10.88	18.4	0.349	4	15

Table 12. 316L SS bilinear stress-strain curve data.

	Temperature (°F)					
	70	200	600	800	1,200	1,400
Elastic modulus (ksi)	28	27	25	23	21	20
Yield strength (ksi)	31	26	19	18	16	15
Tangent modulus (ksi)	400	350	350	350	350	350

Table 13. He-equivalent thermal conductivity.

Temperature (°F)	Thermal Conductivity (Btu/hr-ft-°F)
40	0.085
90	0.091
140	0.096
190	0.102
240	0.107
290	0.112
340	0.117
440	0.126
540	0.136
640	0.145
740	0.153
840	0.162
940	0.17
1,040	0.178
1,140	0.186
1,240	0.194
1,340	0.202
1,440	0.209
1,540	0.217
1,640	0.224
1,740	0.231
1,840	0.238
1,940	0.245
2,040	0.252
2,140	0.258
2,240	0.265
2,340	0.272
2,440	0.278
2,540	0.285
2,640	0.291
2,740	0.297
2,840	0.303
2,940	0.31
3,040	0.316

Table 14. Radiation gap equivalent thermal conductivity.

Temperature (°F)	Thermal Conductivity (Btu/hr-ft-°F)
1,163	0.00303
1,253	0.00356
1,343	0.00415
1,433	0.00481
1,523	0.00553

## APPENDIX B—PROOF TEST RESULTS

The SAFE-100a HX was hydrostatically proof tested to accept the hardware for use in the SAFE-100a pressurized coolant loop system. The target proof pressure was to be held for a minimum of 10 min at a level of  $420\pm 10$  psi, which was determined as follows:

- Design pressure = 200 psi.
- Temperature correction factor =  $Ftu_{\text{test}}/Ftu_{\text{design}}=70/43=1.63$ .
  - Ultimate strength (316L SS) at design temperature (1,200 °F),  $Ftu_{\text{design}}=43$  ksi.
  - Ultimate strength (316L SS) at proof test temperature (70 °F),  $Ftu_{\text{test}}=70$  ksi.
- Proof test factor = 1.25.
- Proof pressure =  $200 \times 1.63 \times 1.25 = 407$  psi (minimum).

The test was performed at MSFC by Propulsion Research Center (TD40) personnel in building 4655 on February 20, 2004. The HX was instrumented with a calibrated pressure transducer and 10 strain gages. Figure 17 shows the test setup. The numbering and locations of the strain gages are shown in figures 18–20. Figure 21 plots the pressure and strain versus time for the test. The pressure was maintained between 410 and 417 psi for a total of 634 s, meeting the targeted pressure and hold time. The HX successfully completed the proof test with no leakage.

A finite element model of the HX was built to analyze the design for the expected test conditions. The proof test was also evaluated with this model. Figure 22 shows the model and the predicted radial strain for a maximum proof pressure of 430 psi. A comparison of the measured strain with the predicted strain at a pressure of 417 psi is shown in figure 23. Overall, with the exception of gages S2001, S2101, and S3003, the measured and predicted strains agree fairly well. The measured strain at these two locations is significantly greater than the predicted level. The strain gradient in these locations is steep and, therefore, sensitive to positional variation. The model uses nominal wall thickness while the as-built wall thickness is unknown. Since the strain in these two locations has a significant bending component, it is sensitive to the wall thickness to the order of  $t^{-2}$ . Therefore, the difference at these locations is not unexpected.

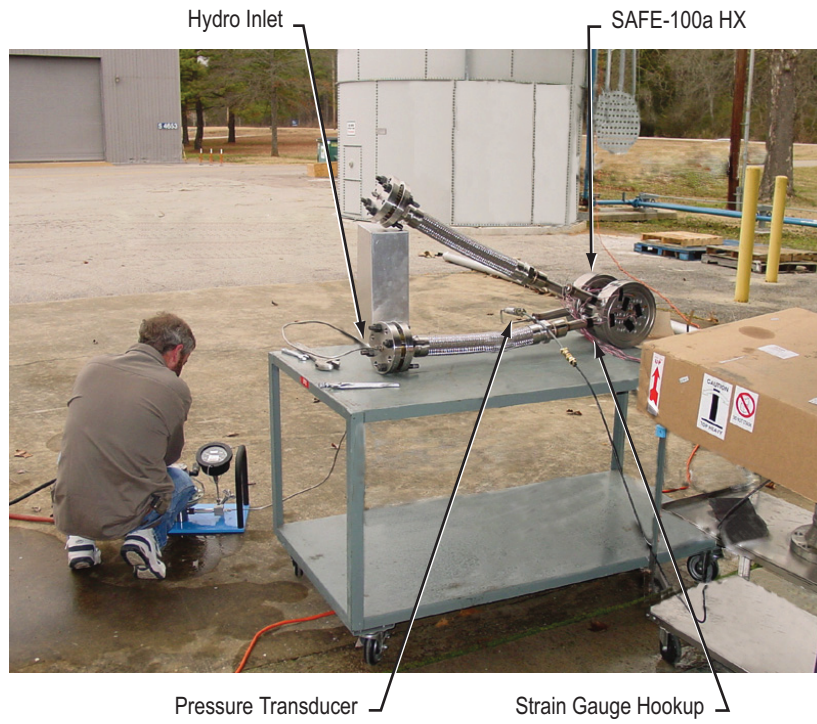


Figure 17. SAFE-100a HX proof test setup.

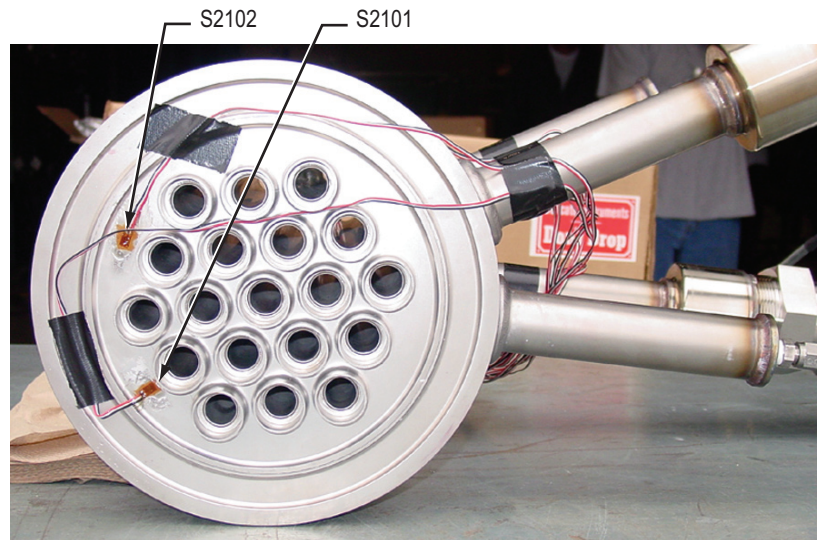


Figure 18. Braze cup side.

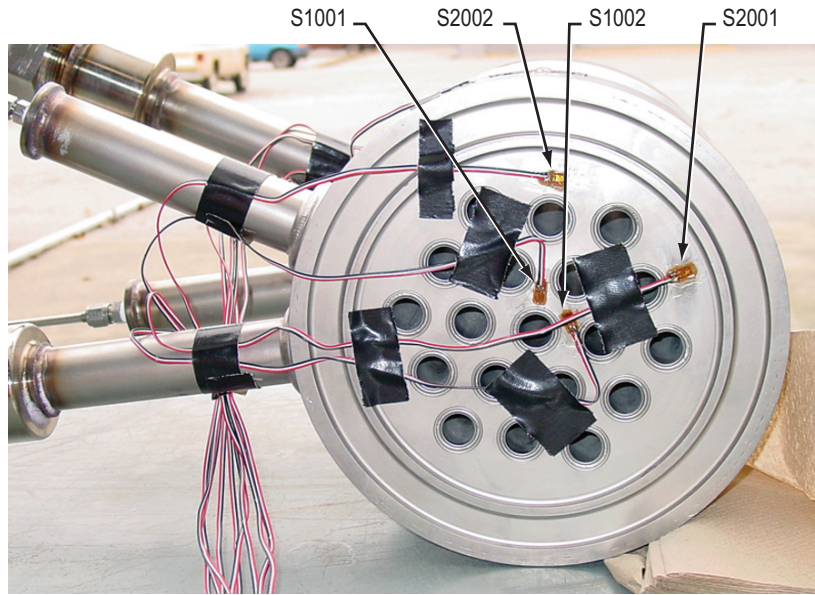


Figure 19. Side opposite braze cups.

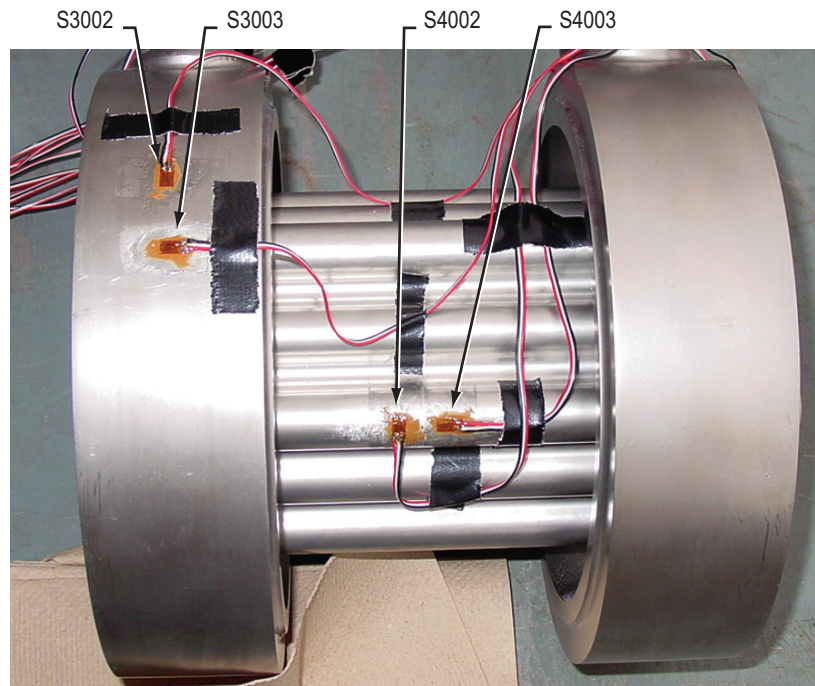


Figure 20. Barrel section.

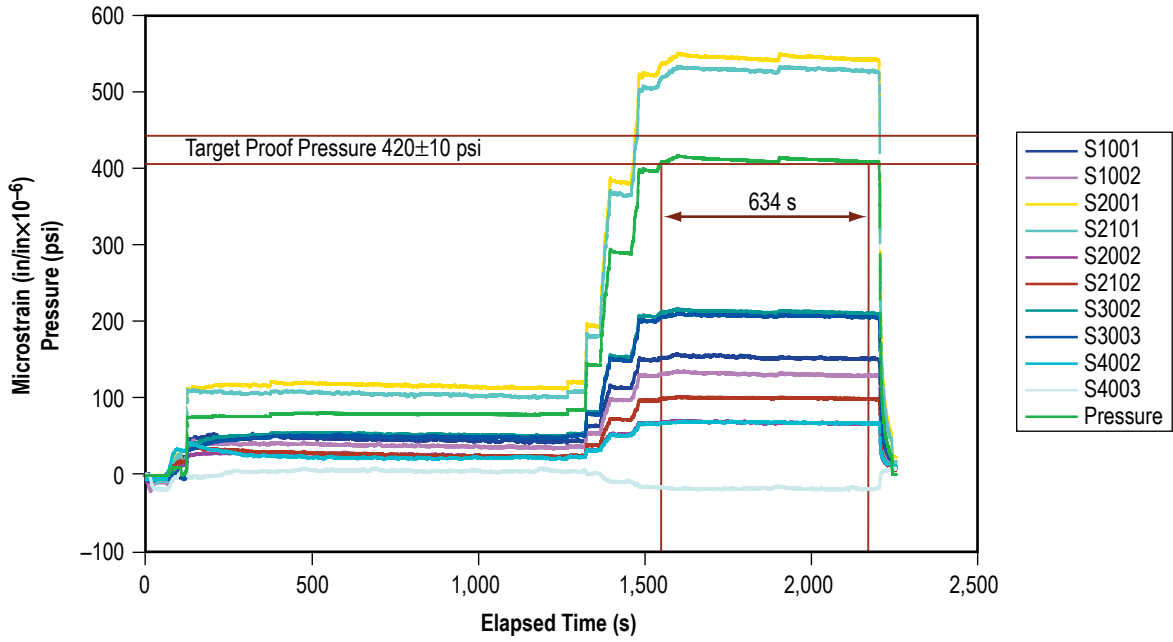


Figure 21. Strains and pressure versus time.

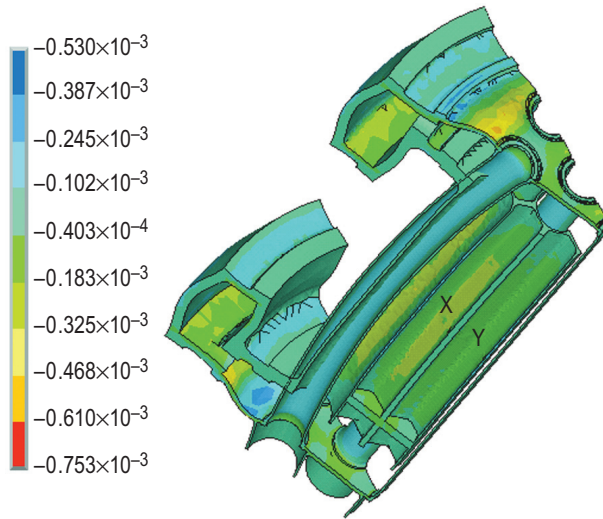


Figure 22. Finite element model radial strain.

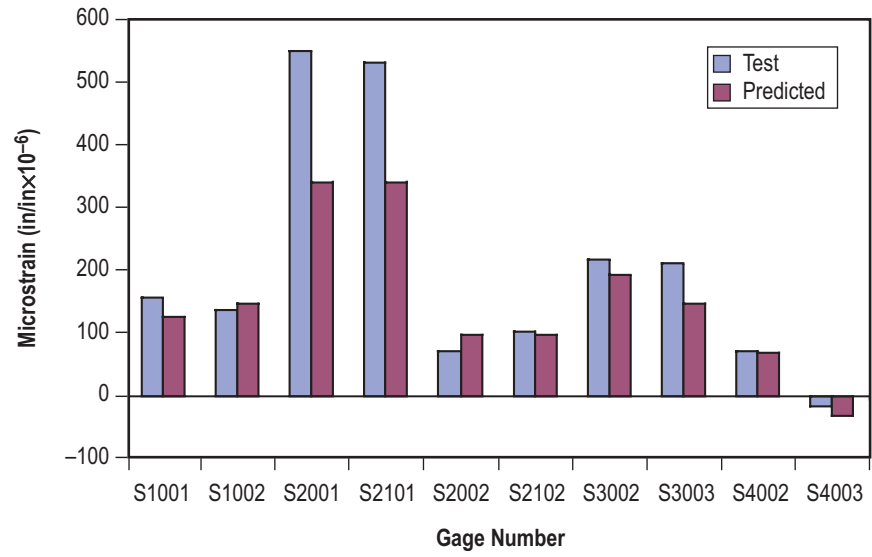


Figure 23. Comparison of test and predicted strain.

## REFERENCES

1. *ASME Pressure Vessel and Boiler Code*, ASME, New York, section III: subsection NH, pp. 26–123, 2001.
2. *Materials Properties Manual*, Rockwell International, Rocketdyne Division, secs. 2211 and 2212, 1986.
3. “Metallic Materials and Elements for Aerospace Vehicle Structures,” *MIL-HDBK-5F*, Government Printing Office, Washington DC, pp. 2-20–2-218, November 1990.
4. “Heat-Transfer Coefficient Calculation for a SAFE-100 Monolithic Braze Heat Exchanger,” *Memorandum ED25-02-25*, Marshall Space Flight Center, November 12, 2002.

REPORT DOCUMENTATION PAGE			Form Approved OMB No. 0704-0188	
Public reporting burden for this collection of information is estimated to average 1 hour per response, including the time for reviewing instructions, searching existing data sources, gathering and maintaining the data needed, and completing and reviewing the collection of information. Send comments regarding this burden estimate or any other aspect of this collection of information, including suggestions for reducing this burden, to Washington Headquarters Services, Directorate for Information Operation and Reports, 1215 Jefferson Davis Highway, Suite 1204, Arlington, VA 22202-4302, and to the Office of Management and Budget, Paperwork Reduction Project (0704-0188), Washington, DC 20503				
1. AGENCY USE ONLY (Leave Blank)	2. REPORT DATE March 2005	3. REPORT TYPE AND DATES COVERED Technical Memorandum		
4. TITLE AND SUBTITLE Safe Affordable Fission Engine- (SAFE-) 100a Heat Exchanger Thermal and Structural Analysis			5. FUNDING NUMBERS	
6. AUTHORS B.E. Steeve				
7. PERFORMING ORGANIZATION NAME(S) AND ADDRESS(ES) George C. Marshall Space Flight Center Marshall Space Flight Center, AL 35812			8. PERFORMING ORGANIZATION REPORT NUMBER  M-1131	
9. SPONSORING/MONITORING AGENCY NAME(S) AND ADDRESS(ES) National Aeronautics and Space Administration Washington, DC 20546-0001			10. SPONSORING/MONITORING AGENCY REPO NUMBER  NASA/TM-2005-213609	
11. SUPPLEMENTARY NOTES Prepared by the Structures, Mechanics, and Thermal Department, Engineering Directorate				
12a. DISTRIBUTION/AVAILABILITY STATEMENT Unclassified-Unlimited Subject Category 39 Availability: NASA CASI 301-621-0390			12b. DISTRIBUTION CODE	
13. ABSTRACT (Maximum 200 words) A potential fission power system for in-space missions is a heat pipe-cooled reactor coupled to a Brayton cycle. In this system, a heat exchanger (HX) transfers the heat of the reactor core to the Brayton gas. The Safe Affordable Fission Engine- (SAFE-) 100a is a test program designed to thermally and hydraulically simulate a 95 Btu/s prototypic heat pipe-cooled reactor using electrical resistance heaters on the ground. This Technical Memorandum documents the thermal and structural assessment of the HX used in the SAFE-100a program.				
14. SUBJECT TERMS heat exchanger, stress analysis, thermal analysis			15. NUMBER OF PAGES 48	
			16. PRICE CODE	
17. SECURITY CLASSIFICATION OF REPORT Unclassified	18. SECURITY CLASSIFICATION OF THIS PAGE Unclassified	19. SECURITY CLASSIFICATION OF ABSTRACT Unclassified	20. LIMITATION OF ABSTRACT  Unlimited	